Journal of Alloys and Compounds 480 (2009) L20–L24

Contents lists available at ScienceDirect

Journal of Alloys and Compounds

journal homepage: www.elsevier.com/locate/jallcom

Letter

Hydrogen uptake of multiwalled carbon nanotubes decorated with Pt–Pd alloy using thermal vapour deposition method

Sang-Woon Hwang, Sami-ullah Rather, Mehraj-ud-din Naik, Chang Su Soo, Kee-Suk Nahm*

Department of Hydrogen and Fuel Cells Engineering, Specialized Graduate School & School of Chemical Engineering, Chonbuk National University, Chonju 561-756, Republic of Korea

ARTICLE INFO

Article history:
Received 21 September 2008
Received in revised form 22 January 2009
Accepted 30 January 2009
Available online 10 February 2009

Keywords:
Nanostructured materials
Vapour deposition
Diffusion
X-ray diffraction
Transmission electron microscopy

ABSTRACT

Hydrogen uptake of Pt–Pd alloy decorated MWCNTs was performed under ambient temperature and moderate pressures. Nanocrystalline alloy is coated on the MWCNTs via thermal vapour deposition (TVD) method. The size of the Pt–Pd alloy decorated by TVD on MWCNTs is 5 nm. The maximum reversible hydrogen storage exhibited by nanocomposite, measured at 298 K and pressure of 20 atm is found to be ~2.0 wt.%, which is nearly 3 times more as compared to pristine CNTs performed under similar experimental conditions. The improvement of hydrogen storage in coated sample as compared to pristine CNTs is due to the spillover of physisorbed hydrogen from the alloy nanoparticles to the CNTs.

1. Introduction

Hydrogen is considered as the ideal fuel and versatile energy carrier. Its advantages in the form of easy to produce, convenient fuel for transportation, converts easily to other forms, high utilization efficiency, and environmental friendliness (zero pollution) makes hydrogen as the alternative fuel in the near future [1–4]. The US Department of Energy (DOE) hydrogen plan has set a standard by providing a commercially significant benchmark for the amount of reversible hydrogen adsorption. The benchmark requires a system-weight efficiency of 6.5 wt.% hydrogen and a volumetric density of 62 kg H_2/m^3, since a vehicle powered by a fuel cell would require 3.1 kg of hydrogen for a 500 km range [5–9].

Discovery of carbon nanotubes by Iijima in 1991 makes the carbon nanotubes very interesting material for hydrogen storage, as it can store hydrogen inside the channels of the carbon nanotubes and also due to its high surface area, it can accommodate large number of hydrogen [10]. Till now carbon nanotubes alone cannot satisfy the target set by the DOE. Scientists believe that modification of carbon nanotubes in terms of purification and coating with transition or transition metal oxide nanoparticles can satisfy the target of DOE. During hydrogenation of coated carbon nanotubes, a very interesting mechanism emerges called spillover mechanism. Metal nanoparticles dissociate the hydrogen molecule and spill it over the carbon nanotubes [11,12]. The hydrogen binding characteristics and the geometry of transition metal adatoms, such as Ti, Sc, Pt, and Pd dispersed on fullerene, carbon nanotubes, and other aromatic hydrocarbons determined using density functional calculations and unique enhancement of hydrogen storage capacities in metal-decorated carbon nanotubes [13–17]. This hybridization involves $3c–2e^-$ bonds where the molecular hydrogen is directly bonded to metal center and is known as Kubas interaction, after the pioneering work by Gregory Kubas in 1984. The presence of vacant metal d-orbitals of suitable energy is of paramount importance for the stabilization of Kubas complexes [18,19]. Zacharia et al. reported that platinum nanoparticles deposited on carbon nanotubes by sputtered deposition method enhance the hydrogen storage capacity more than 40 times as compared to purified carbon nanotubes performed under the similar conditions [20]. The enhancement of storage capacity is due to the spillover of hydrogen from Pt nanoparticles to carbon nanotubes. Spillover mechanism is active only when majority of metal nanoparticles are exposed to hydrogen during the adsorption process. However, if the metal nanoparticles are inside the channels of carbon nanotubes, there are less chances of spillover effect [21]. It is believed that doping of transition metals into carbon nanotubes narrows the gap of DOE target for commercial purposes. Till now transition metals like Pt, Pd, Ni, Mg, etc. were doped into purified carbon nanotubes by incipient wetness impregnation, in situ reduction, high-energy ball milling, sputtering, and electrochemical methods [21–24]. Inspired by these findings, we here aim to understand the decoration of Pt–Pd alloy on pristine carbon nanotubes by thermal vapour deposition (TVD)

---

* Corresponding author. Tel.: +82 63 270 2311; fax: +82 63 270 3908.
E-mail address: nahmks@chonbuk.ac.kr (K.-S. Nahm).

0925-8388/$ – see front matter © 2009 Elsevier B.V. All rights reserved.
doi:10.1016/j.jallcom.2009.01.136

method, and also effect of doping on hydrogen storage capacity at room temperature and a hydrogen pressure technically relevant for hydrogen storage commercially.

Here, we report the hydrogen storage characteristics of platinum–palladium alloy decorated multiwalled carbon nanotubes measured at an ambience of 298 K and a hydrogen pressure range of 20–32 atm. The Pt–Pd nanoparticles are decorated on the multiwalled carbon nanotubes via thermal vapour deposition method. The hydrogen storage capacity of the coated sample is compared with the pristine carbon nanotubes measured under similar experimental conditions using Sievert's volumetric apparatus. The main aim of this paper is to decorate the pristine carbon nanotubes with metal alloy nanoparticles to facilitate the spillover mechanism.

2. Experimental

Multiwalled carbon nanotubes with diameter 10–40 nm obtained from CNT Corporation, were purified prior to use for the deposition of metal nanoparticles. The metallic and amorphous carbon impurities in the as purchased samples were reduced to less than 2 wt.% by subjecting them to a sequential acid-treatment and hydrogen-etching at 973 K [25]. The platinum–palladium coated MWCNTs were synthesized by a thermal vapour deposition method equipped with a 0.3-mm thick Pt–Pd alloy source. In a typical thermal vapour deposition experiment, approximately 80 mg of carbon nanotube was uniformly spread on the sample holder. Prior to the deposition, the chamber was evacuated to a base pressure of 1×10^{-6} Torr. When the pressure in the chamber remained stable, current (200 mA) is passed through the sample for 200–300 s. After the experiment, the chamber was vented and the samples were collected. The crystal structure of Pt–Pd coated MWCNT composite was examined using Rigaku D/MAX 2500 X-ray diffractometer equipped with a Cu-Kα radiation source ($\lambda = 0.15418$ nm). The samples for XRD measurement were prepared by vacuum drying at 373 K. Field emission electron microscopy (Hitachi, S-4700) and transmission electron microscopy (JEOL JEM 2010) data were used to determine the size and morphology of alloy coated CNTs. The specific surface area of pristine and coated samples was determined by the Brunauer–Emmett–Teller (BET) N_2 adsorption isotherm technique (BEL Japan Inc.).

Transient hydrogen adsorption studies of Pt–Pd alloy coated CNTs were performed by using Sievert's volumetric equipment at RT and a hydrogen pressure of 20 and 32 atm. Prior to the hydrogen storage experiments, we performed the determination of the dead-volume of the system using the helium gas. The determined volume was additionally cross-checked using the hydrogen adsorption data of a known amount of the intermetallic alloy $LaNi_5$ [26]. Nearly 50 mg of sample was used in each storage experiment. Prior to each adsorption experiment, the samples were out-gassed for nearly 3 h by heating to 473 K under continuous evacuation up to 10^{-4} Torr. The gravimetric storage capacity of Pt–Pd/CNT composite material was determined from the pressure drop of hydrogen gas using the ideal gas equation. Additional re-adsorption experiments were performed on previously adsorbed samples after degassing the samples at 473 K for nearly 4 h. Data acquisition for hydrogen storage was automated by interfacing the pressure transducer output to a PC via RS-232 device. Further experimental details can be obtained from elsewhere [26].

3. Results and discussion

Fig. 1 displays the XRD profile of Pt–Pd alloy coated carbon nanotube composite synthesized by thermal vapour deposition method before and after hydrogenation. The peaks in the spectra correspond to the reflections from (1 1 1) and (2 2 0) lattice planes of cubic Pt–Pd alloy with the space group of F*m*3*m* (JC-PDS PD File No. 03-065-6418). A peak that appeared at 26.34° and 43.37° indicates the reflection from (0 0 2) and (0 1 2) lattice of graphite with the space group of F*m*3*m* (JC-PDS PD File No. 00-001-0640 and 01-089-8490). All the peaks of Pt–Pd alloy are broader indicating the smaller size of particles. The Pt–Pd alloy peaks almost disappear after the hydrogenation of the sample. The size of the coated metal particles determined by Scherrer formula is found to be between 4 and 6 nm [27]. The size of the Pt–Pd alloy particles decorated on the MWCNTs was initially controlled to 5 nm by using the thermal vapour deposition method.

The morphology of pristine and Pt–Pd coated carbon nanotubes analyzed by field emission scanning electron microscope (FESEM) is provided in Fig. 2a–c. The Pt–Pd coating is visible on the carbon nanotube samples. Panels 'b' and 'c' provided the FESEM images of Pt–Pd coated CNT before and after hydrogenation, respectively.

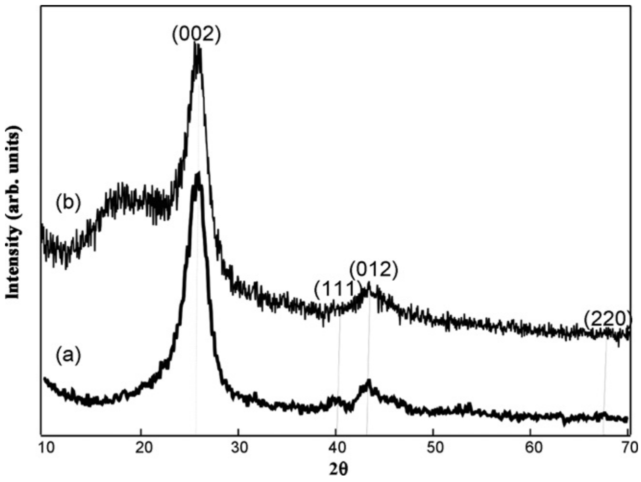

Fig. 1. X-ray diffraction pattern of Pt–Pd coated carbon nanotubes synthesized by the thermal vapour deposition method before (a) and after (b) hydrogenation.

The larger Pt–Pd particles coated on the carbon nanotubes after hydrogenation as compared to prior hydrogenation is due to the agglomeration of particles after number of cycles of adsorption/re-adsorption as shown in the panel 'c'. The energy dispersive X-ray (EDX) response of the Pt–Pd alloy coated carbon nanotube samples averaged over several randomly chosen sample regions plotted in Fig. 2d, shows the peaks corresponding to elemental carbon, platinum, and palladium.

The BET specific area of pristine carbon nanotubes is found to be 284 m^2/g, however the surface area decreases to 216 m^2/g after decorating the carbon nanotubes with Pt–Pd alloy. The decrease in surface area is due to the blocking of pores and channels of carbon nanotubes by Pt–Pd alloy nanoparticles synthesized by thermal vapour deposition method [23].

Hydrogen storage characteristics of platinum–palladium coated carbon nanotube composites are provided in Fig. 3. The maximum hydrogen storage capacity of coated carbon nanotube samples measured at 298 K and a hydrogen pressure of 20 atm is found to be ∼2.0 wt.% (panel 'A'). The hydrogen storage capacity of coated CNTs averaged over several storage experiments is found to be ∼2.0 wt.%, nearly more than 3 times larger when compared with the pristine carbon nanotube samples (not displayed here). The enhancement of more than 3 times is due to the interfacial diffusion of hydrogen from Pt–Pd nanoparticles to the carbon nanotube surface called spillover mechanism (Fig. 5d). The spillover mechanism is experimentally observed using the hydrogen storage capacity of coated carbon nanotubes ($\text{wt.\%}_{\text{Pt-Pd/CNT}}$) as a linear combination of the hydrogen storage capacities of Pt–Pd nanoparticles, pristine carbon nanotubes, and spillover of atomic hydrogen from the nanoparticles to the carbon nanotubes.

$$\text{wt.\%}_{\text{Pt}-\text{Pd/CNT}} = \text{wt.\%}_{\text{Pt}-\text{Pd}} + \text{wt.\%}_{\text{CNT}} + \text{wt.\%}_{\text{S}}$$

Here, $\text{wt.\%}_{\text{Pt-Pd/CNT}}$, $\text{wt.\%}_{\text{CNT}}$, and $\text{wt.\%}_{\text{S}}$ represent the hydrogen storage capacities of Pt–Pd alloy nanoparticles, pristine carbon nanotubes, and spillover phenomenon, respectively. Prior activation, the hydrogen storage capacity is found to be 0.63 wt.% at 298 K and a hydrogen pressure of 32 atm. Hydrogen storage capacity increases sharply after activated the sample at 473 K in the presence of hydrogen for 2 h. The maximum hydrogen storage capacity reaches to 1.85 wt.% at 298 K and a hydrogen pressure of 32 atm. The hydrogen storage capacity increases further to 2.0 wt.% which is more than 3 times as compared to purified carbon nanotubes at 298 K and a hydrogen pressure of 20 atm after number of cycles of adsorption/re-adsorption. Activation at 473 K in presence of hydrogen makes the sample smaller and creates defects

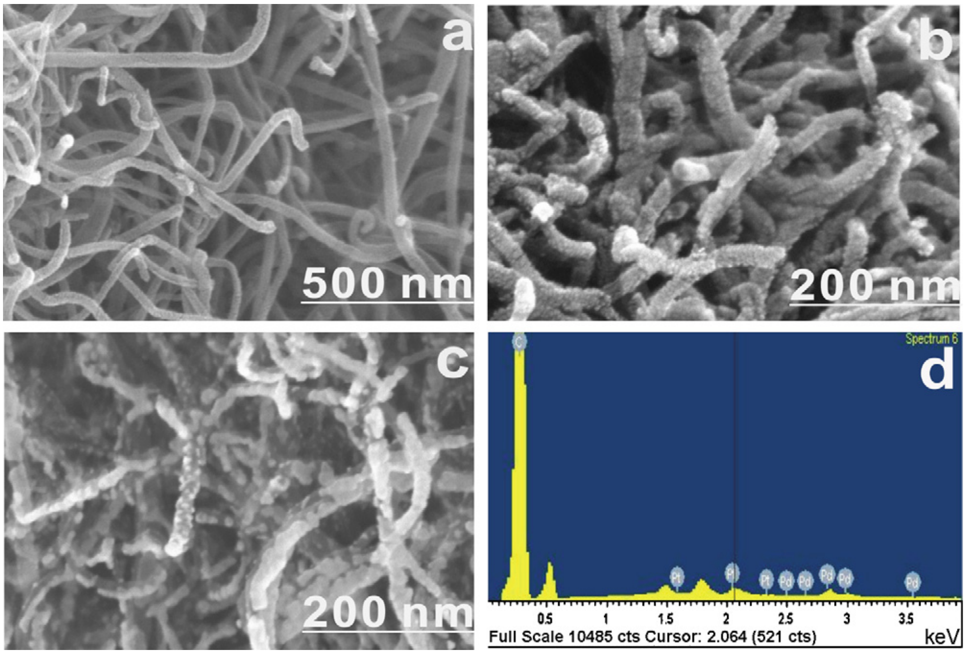

Fig. 2. Field emission scanning electron microscopy (FESEM) images of (a) pristine CNTs, (b) and (c) Pt–Pd coated CNTs before and after hydrogenation, respectively. The panel 'd' of the Pt–Pd coated CNT prior hydrogenation gives the energy dispersive X-ray response averaged over several sample regions.

which facilitate the spillover of hydrogen from metal nanoparticles to carbon nanotubes. As shown in Fig. 3a, the hydrogen storage capacity shows slow kinetics without activation. Adsorption kinetics increases sharply as the number of activation cycles increases ('b' and 'c'). As shown in Fig. 4a the metal nanoparticles are very close on the surface of carbon nanotubes make it difficult for the metal particles to dissociate the hydrogen molecule and spill them to carbon nanotubes. The hydrogen storage capacity increases to ~2.0 wt.% at 20 atm as compared to 32 atm. Hydrogen adsorption decreases from ~2.0 wt.% (Fig. 3b) to 1.90 wt.% (Fig. 3a) after successive cycles of adsorption/readsorption at RT and 20 atm (panel 'B'). The diminishing hydrogen storage capacity is due to the increasing size of metal particles by agglomeration confirmed by the TEM images as well as particle size distribution (PSD) [28].

Representative TEM images presented in Fig. 4a–c indicate the nanostructural characterization of the Pt–Pd coated carbon nanotube samples. Here, the panel 'a' corresponds to the Pt–Pd coated CNT sample prior to hydrogenation, 'b' to the coated sample after hydrogenation, and 'c' after the 10th cycle of adsorption/re-adsorption. TEM images suggest that the Pt–Pd alloy nanoparticles mostly are attached to the walls of carbon nanotubes and are not localized within the nanotubes. It can be understood that the Pt–Pd nanoparticles can be coated on the nanotubes using the thermal vapour deposition method. Platinum–palladium alloy nanoparticles coated on the carbon nanotubes have size 5 nm that can be controlled during the thermal vapour deposition process. As it is evident from the TEM images that after successive adsorption/re-adsorption cycles, the particle size increases due to the agglomeration. The histogram shows that the particle size distribution (PSD) of the Pt–Pd coated sample after successive cycles of hydrogenation is constructed by sampling TEM image (panel 'd'). The average size of the particle is 9.73 nm with a standard deviation (σ) of 2.75 nm. The average size of metal nanoparticles after hydrogenation increases more than double as compared to prior

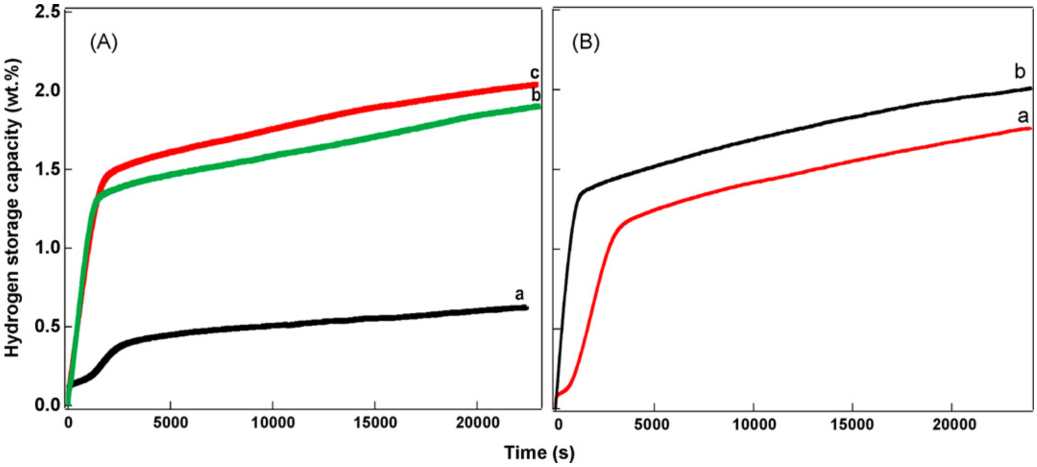

Fig. 3. Hydrogen storage capacity of Pt–Pd alloy coated MWCNTs measured at 298 K and moderate pressures. Panel 'A' provided the hydrogen storage capacity at (a) 32 atm (no activation), (b) 32 atm (activation), and (c) 20 atm (after successive adsorption/re-adsorption cycles. Panel 'B' provides the hydrogen adsorption cycles after successive adsorption and desorption cycles at RT and 20 atm.

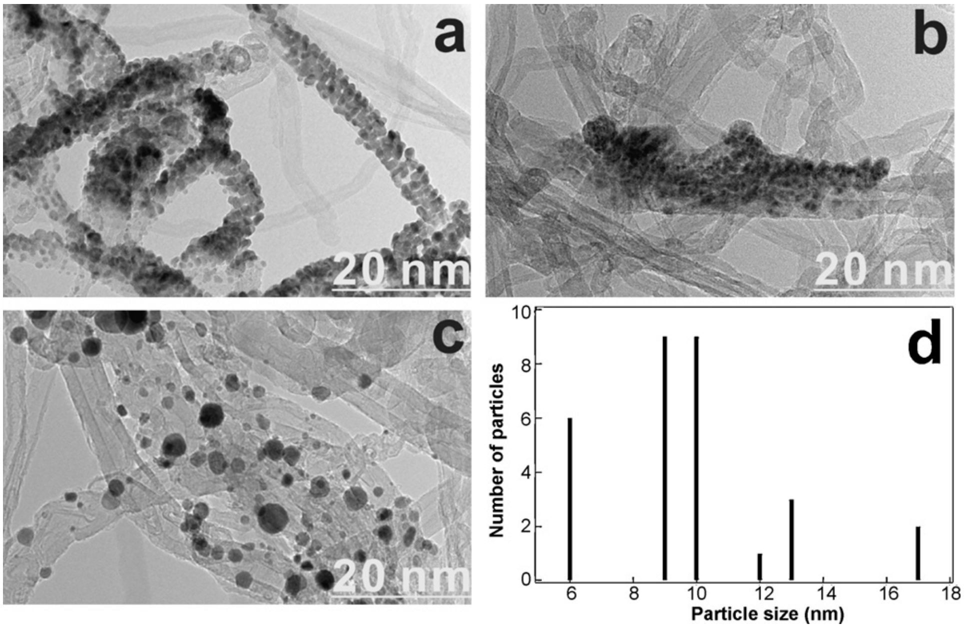

Fig. 4. Representative transmission electron microscope images of Pt–Pd coated carbon nanotubes before and after hydrogenation: (a) prior hydrogenation, (b) and (c) after hydrogenation for number of adsorption and desorption cycles. The panel 'd' provides the histogram of particle size distribution corresponding to the sample (c).

hydrogenation of the Pt–Pd coated carbon nanotube samples. This sharp increase of metal particle size is due to the agglomeration occurring during the continuous adsorption/re-adsorption cycles.

The schematic illustration of the formation of agglomeration during and after the successive hydrogenation cycles on the coated carbon nanotubes is shown in Fig. 5. Initial hydrogenation first decreases the size of the particles (b) and then successive cycles of adsorption/re-adsorption increases the size of the metal particles due to the agglomeration (c). During step (b) the binding energy first decreases slowly as the hydrogen gets closer to the nanotubes and Pt–Pd alloy. The H_2 molecule is attracted to the metal alloy with a sudden decrease in the energy. The decrease in energy is achieved by dissociating the hydrogen molecule into 2 hydrogen atoms. At this point, the H–H distance increases from 0.86 to 2.71 Å. The interaction between H_2 and alloy is always attractive and therefore H_2 is adsorbed onto the Pt–Pd alloy without any energy barrier and subsequently spills them over to the carbon nanotubes (d) [29,30].

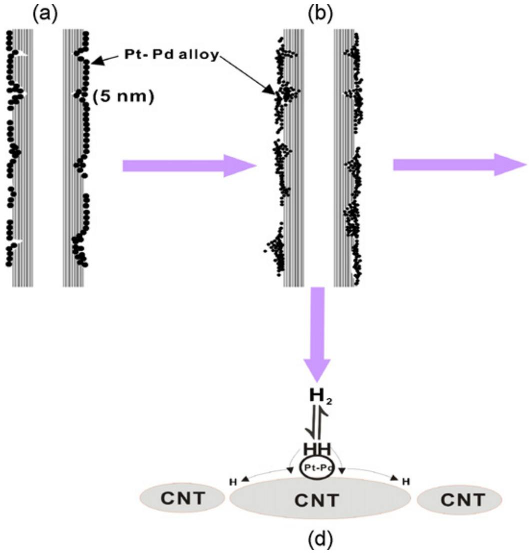

Fig. 5. Schematic diagram of agglomeration of metal nanoparticles during the hydrogenation cycles. (a) Corresponds to the Pt–Pd coated carbon nanotubes before hydrogenation, (b) during hydrogenation, and (c) after successive number of adsorption/re-adsorption cycles. (d) Spillover of atomic hydrogen dissociated by the platinum–palladium alloy nanoparticles to the pristine carbon nanotube.

4. Conclusion

The hydrogen storage studies of platinum–palladium decorated CNTs synthesized by thermal vapour deposition method have been investigated using the Sievert's volumetric apparatus. It was found that the hydrogen storage capacity of the coated carbon nanotube samples measured at 298 K and moderate hydrogen pressure was enhanced by nearly 3 times when compared with the storage capacity of the pristine samples performed under the similar experimental conditions. The enhanced hydrogen storage capacity of more than 2.0 wt.% is due to the spillover of hydrogen from the Pt–Pd alloy nanoparticles to the carbon nanotubes. The hydrogen storage capacity increases from 0.63 to 2.0 wt.% at RT and a hydrogen pressure of 20 atm after activation of sample at 473 K in presence of hydrogen for 2 h.

Acknowledgment

This work was supported by the Ministry of Knowledge Economy (MKE) through the Specialized Graduate School Program.

References

[1] W. Qikun, Z. Changchun, L. Weihua, W. Ting, Int. J. Hydrogen Energy 27 (2002) 497.
[2] Y.J. Choi, J. Lu, H.Y. Sohn, Z.Z. Fang, J. Power Sources 180 (2008) 491.
[3] C.H. Chen, C.C. Huang, Micropor. Mesopor. Mater. 109 (2008) 549.
[4] A.L.M. Reddy, S. Ramaprabhu, Int. J. Hydrogen Energy 33 (2008) 1028.
[5] M. Sankarana, B. Viswanathan, S.S. Murthy, Int. J. Hydrogen Energy 33 (2008) 393.
[6] P. Benard, R. Chahine, P.A. Chandonia, D. Cossement, G.D. Douville, L. Lafi, P. Lachance, R. Paggiaro, E. Poirier, J. Alloys Compd. 446–447 (2007) 380.
[7] W.C. Xu, K. Takahashi, Y. Matsuo, Y. Hattori, M. Kumagai, S. Ishiyama, K. Kaneko, S. Iijima, Int. J. Hydrogen Energy 32 (2007) 2504.
[8] C. Weng, S.P. Ju, K.C. Fang, F.P. Chang, Comput. Mater. Sci. 40 (2007) 300.
[9] P. Benard, R. Chahine, Scripta Mater. 56 (2007) 803.
[10] S. Iijima, Nature 354 (1991) 56.
[11] F.H. Yang, A.J. Lachawiec Jr., R.T. Yang, J. Phys. Chem. B 110 (2006) 6236.

[12] P. Chen, X. Wu, J. Lin, K.L. Tan, Science 285 (1999) 91.
[13] T. Yildirim, S. Ciraci, Phys. Rev. Lett. 94 (2005) 175501.
[14] T. Yildirim, J. Iniguez, S. Ciraci, Phys. Rev. B 72 (2005) 153403.
[15] S. Dag, Y. Ozturk, S. Ciraci, T. Yildirim, Phys. Rev. B 72 (2005) 155404.
[16] Y. Zhao, Y.H. Kim, A.C. Dillon, M.J. Heben, S.B. Zhang, Phys. Rev. Lett. 94 (2005) 155504.
[17] X.L. Wang, J.P. Tu, Appl. Phys. Lett. 89 (2006) 064101.
[18] G.J. Kubas, R.R. Ryan, B.I. Swanson, P.J. Vergamini, H.J. Wasserman, J. Am. Chem. Soc. 106 (1984) 451.
[19] G.J. Kubas, J. Organomet. Chem. 635 (2001) 37.
[20] R. Zacharia, S.U. Rather, S.W. Hwang, K.S. Nahm, Chem. Phys. Lett. 434 (2007) 286.
[21] S.U. Rather, R. Zacharia, S.W. Hwang, M. Naik, K.S. Nahm, Chem. Phys. Lett. 441 (2007) 261.
[22] C.Z. Wu, P. Wang, X. Yao, C. Liu, D.M. Chen, G.Q. Lu, H.M. Cheng, J. Alloys Compd. 420 (2006) 278.
[23] R. Zacharia, K.Y. Kim, A.K.M.F. Kibria, K.S. Nahm, Chem. Phys. Lett. 412 (2005) 369.
[24] C.T. Hsieh, Y.W. Chou, W.Y. Chen, J. Alloys Compd. 466 (2008) 233.
[25] P.X. Hou, Q.H. Yang, S. Bai, S. Xu, M. Liu, H.M. Cheng, J. Phys. Chem. B 106 (2002) 963.
[26] S.U. Rather, R. Zacharia, S.W. Hwang, M.D. Naik, K.S. Nahm, Chem. Phys. Lett. 441 (2007) 261.
[27] E.A. Baranova, Y.L. Page, D. Ilin, C. Bock, B. MacDougall, P.H.J. Mercier, J. Alloys Compd. (2008) 101, doi:10.1016/j.jallcom.2008.03.101.
[28] Q. Sun, Q. Wang, P. Jena, Y. Kawazoe, J. Am. Chem. Soc. 127 (2005) 14582.
[29] M. Sankaran, B. Viswanathan, Carbon 44 (2006) 2816.
[30] M. Zielinski, R. Wojcieszak, S. Monteverdi, M. Mercy, M.M. Bettahar, Catal. Commun. 6 (2005) 777.